Supramolecular Polymerization of all-*cis*-Fluorinated Cyclohexanes: Influence of Side Chains

Shyamkumar V. Haridas[a]
Oleksandr Shyshov[a]
Max von Delius * [a]
[a] Institute of Organic Chemistry, Ulm University, Albert-Einstein-Allee 11, 89081 Ulm, Germany
* max.vondelius@uni-ulm.de

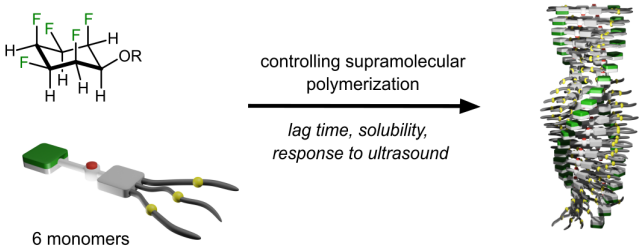

Received: 28.05.2023
Accepted after revision: 27.07.2023
DOI: 10.1055/s-0043-1761314; Art ID: OM-2023-05-0003-OA

Abstract Custom-designed materials based on supramolecular polymers are of interest for applications in organic electronics and biomedicine. Recently, we have shown that derivatives of the highly polar compound all-*cis* hexafluorocyclohexane undergo seeded polymerization and can therefore be used to prepare soluble nanofibers with controlled length. In this work, we aimed to explore the scope of this process. We studied the supramolecular polymerization of six all-*cis*-fluorinated cyclohexane monomers, with five differing in the solubilizing side chains and one in the secondary supramolecular binding site. In studies on controlled supramolecular polymerization, we found that three of the monomers could be induced to polymerize by ultrasound irradiation and four by addition of seeds. For these latter examples, we were able to identify a solvent mixture that led to spontaneous polymerization and hysteresis in heating and cooling curves. These results show that the living supramolecular polymerization of fluorinated cyclohexanes is not limited to one particular monomer, but that side chains exhibiting a strong solvophobic effect that cannot be compensated within the binary solvent "window" represent a limitation to the approach. We also demonstrate that nanofibers based on stacks of fluorinated cyclohexanes can be dissociated by addition of chloride ions.

Key words: supramolecular polymers, seeded polymerization, C–H hydrogen bonds, CD spectroscopy

Introduction

The ability to endow synthetic polymers with custom-designed properties is one of the cornerstones of modern materials science. A common strategy to achieve this end is to modify the side chain(s) in the monomer such that the final polymer exhibits the desired solubility, stability or other characteristics relevant to the material's purpose. In the past two decades, supramolecular polymers[1] have received attention due to their unique properties such as degradability and stimuli-responsiveness.[2] Similar to covalent polymers, modification of side chains impacts both the polymerization process and the material properties.[3] For instance, Meijer and co-workers have extensively studied variations of supramolecular polymers based on the benzenetricarboxamide (BTA)[4] core, and made use of a tailored side chain to self-assemble a magnetic resonance imaging contrast agent.[5] Another interesting example for the strategic design of side chains is "Archimedean spirals"[6] that are obtained thanks to perfluorinated alkyl chains.

Following advances on the living epitaxial growth of block copolymers,[7] "living supramolecular polymerization" (LSP)[8] has become an active area of research, because it enables control over the length of fibres and in some instances even the preparation of block copolymers.[9] LSP was first reported in 2014 by the group of Takeuchi and Sugiyasu[10] by utilizing different aggregation pathways[11] of a porphyrin-based monomer. Several reports of LSP made use of this strategy of adding seeds of thermodynamically stable fibres to kinetically trapped on/off-pathway aggregates.[12] Another approach for realising LSP is to design kinetically trapped monomers which are unable to polymerize spontaneously but are capable of forming thermodynamically stable polymers by adding seeds.[13] Further reports describe LSP triggered by chemical fuels or light.[14]

Recently, our group reported the LSP of fluorinated cyclohexanes[15] by utilizing the large dipole moment of all-*cis* hexafluorocyclohexane (Figure 1).[16] The $C_6H_6F_6$ molecule holds promise for supramolecular chemistry and materials science,[17] because of its dipole moment (5.7 Debye; largest known for an aliphatic molecule) and its ability to bind anions.[18] We showed that the molecule **M-3** (Scheme 1) in a carefully chosen binary solvent mixture (84 : 16 cyclohexane : $CHCl_3$, 1.2 mm) adopts a kinetically trapped folded state that inhibits spontaneous polymerization. By adding well-defined seeds to such a monomer solution, we were able to induce well-behaved LSP and obtain soluble nanofibers with controlled length (Figure 1). We have also utilized these kinetically trapped monomers to create supramolecular block copolymers comprising monomers **M-3** and **M-5**.

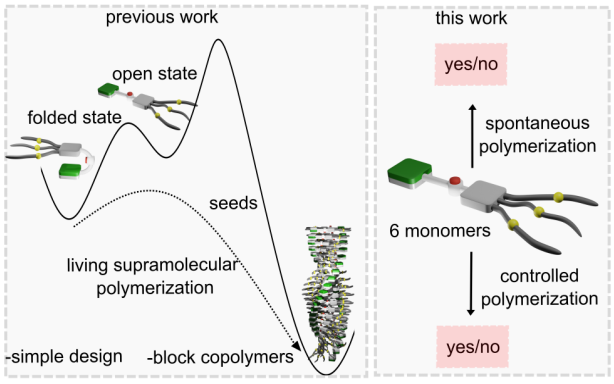

Figure 1 Scope of this study and molecular design. Green domain: all-*cis*-fluorinated cyclohexane; red domain: secondary supramolecular binding motif (amide/urea); yellow domain: thioether linkage offering straightforward modulation of side chain structure.

Herein, we study a total of six structurally related monomers (**M-3, M-5–9**) to shed light on the scope of LSP and the underlying supramolecular chemistry. Five of the investigated molecules differ by their side chains (**M-3, M-5–8**), while one (**M-9**) differs by the presence of a urea instead of an amide secondary binding site. We show that these structural changes affect (i) the solvent composition needed to create kinetically trapped monomer solutions, (ii) the lag time before spontaneous polymerization or precipitation occurs and (iii) the ability to perform LSP.

Results and Discussion

Synthesis

The syntheses of monomers **M-6, M-7**, and **M-8** were carried out by first converting citronellol (**1**) via alcohols **2** and **3** into the three-fold iodinated derivative **4**. This modular route allows the convenient attachment of different side chains by nucleophilic substitution with commercially available thiols (**5**, Scheme 1). In the two final steps of the synthesis, an active ester was installed (**6**), followed by amide bond formation with the crucial mono-functionalized all-*cis*-fluorinated cyclohexane whose synthesis was described previously.[15] In this way, we obtained the following new monomers that differ significantly in their side chains: **M-6** containing a terminal isopropyl group, **M-7** containing a highly fluorinated alkyl chain (C_6F_{13}) and **M-8** carrying a benzyl group. The syntheses of monomers **M-3** and **M-5** were reported previously.[15] Compound **M-9**, which differs from **M-3** by the replacement of an amide motif with a urea motif, was synthesized using a different route. First, we converted gallic acid derivative **7** into the corresponding isocyanate **9** by making use of the Curtius rearrangement in the key step.

General Approach for Supramolecular Polymerization Studies

We describe here general considerations for this comparative study on the polymerization of monomers **M-3** and **M-5–9**. Following a discussion of results obtained with indi-

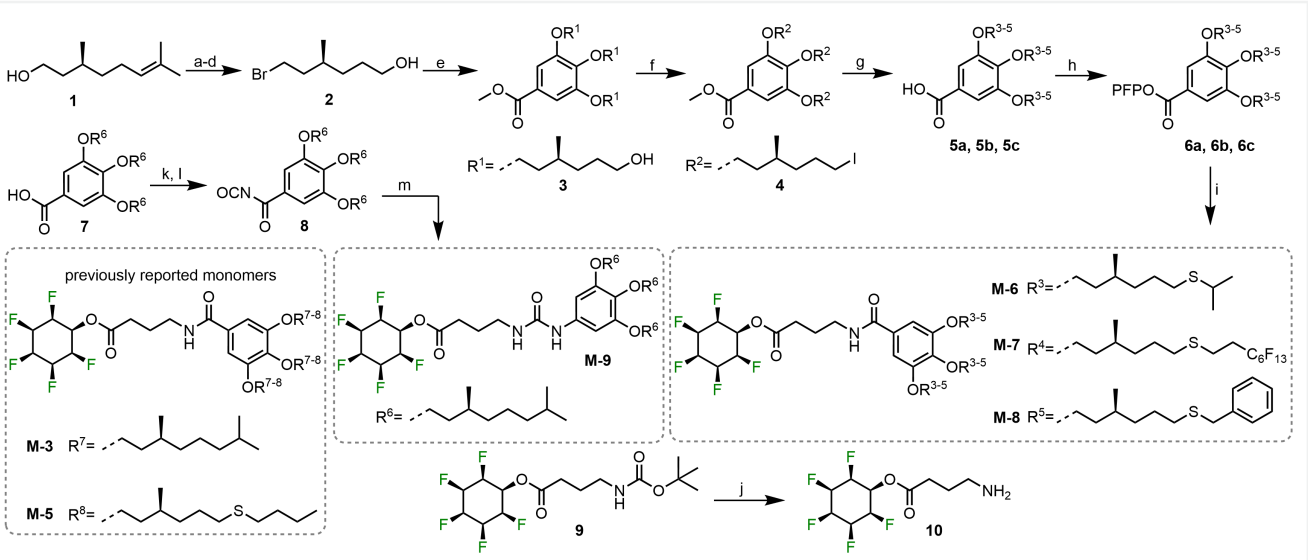

Scheme 1 a) Br_2, PPh_3, pyridine, DCM, 0 °C to rt, 18%. b) *m*CPBA, DCM, 0 °C to rt. c) $NaIO_4$, H_2SO_4, dioxane, rt. d) $NaBH_4$, DMF, 0 °C to rt, 46%. e) Methyl gallate, Cs_2CO_3, DMF, 130 °C, 65%. f) I_2, PPh_3, imidazole, acetonitrile, 0 °C to rt, 68%. g) Cs_2CO_3, TBAI, DMF, RSH (**5a, 5b**, and **5c** denote compounds with R = isopropyl, $C_8H_4F_{13}$ and benzyl, respectively). h) Pentafluorophenol (PFP-OH), EDC.HCl, DMAP, DCM, i) **10**, DIPEA, DCM, j) TFA, DCM, k) PPh_3, CCl_3CN, NaN_3, acetonitrile, l) toluene, reflux, m) **10**, DIPEA, DCM. Monomer numbering starts with **M-3** and **M-5** for consistency with a previous report.[15]

vidual monomers, we return to a comparative discussion in the Conclusion section of this article (with a comparative table).

All polymerization experiments were performed in binary mixtures of cyclohexane and chloroform, such that reliable comparisons can be drawn. Monomers were first allowed to polymerize spontaneously, and the polymerization was monitored by electronic circular dichroism (CD) spectroscopy. Where applicable, the morphology of nanofibers was probed and visualized by atomic force microscopy (AFM). To monitor the supramolecular polymerization from these kinetically trapped (folding[15]) monomers over a convenient timescale, we decided to keep the lag time within 2 hours. We were able to do this by tuning the composition of the binary solvent mixture. A higher proportion of the "antisolvent" cyclohexane generally shortens the lag time. The combination of lag time and solvent composition therefore allows drawing conclusions on the solvophobic effect that is experienced by the monomers/polymers. Once an ideal solvent composition was identified for spontaneous polymerization, we conducted variable-temperature CD spectroscopy to understand the kinetic influence on supramolecular (de)polymerization. A hysteresis curve in the cooling and heating cycles is the indication that the polymerization is governed by kinetic control. In our previous study, we found out that by applying ultrasound or by adding seeds, it was possible to induce **M-3** to polymerize.[15] We decided to attempt this controlled polymerization with the new monomers as well in a solvent composition higher in chloroform content to make sure the polymerization can be induced by a stimulus and does not occur spontaneously. In such a study, polymerization was initiated by sonication and such nanofibers were used as seeds to initiate polymerization of a solution of monomers in a monomer to seed ratio of 50 : 1 (in the previously tuned binary solvent mixture).

Insights into Previously Reported Monomers: M-3 (^{i}pr) and M-5 (S^{n}Bu)

M-3 gave rise to seeded (living) supramolecular polymerization in the 84 : 16 cyclohexane/chloroform solvent system in our previous work.[15] Using **M-5** as a comonomer, we were also able to prepare supramolecular block copolymers by utilizing solvent mixtures in which both monomers did not spontaneously polymerize over many hours (**M-3:** 84 : 16; **M-5:** 93 : 7). We have now studied the spontaneous polymerization of both these monomers in more detail, which required variation of the solvent mixture. By increasing the fraction of the antisolvent in the solvent mixture (**M-3:** 88 : 12; **M-5:** 94 : 6), we were able to observe polymerization within less than 2 hours. As can be seen in the CD data shown in Figure 2 (a, c), the polymerization occurred spontaneously and the heating/cooling curves showed hysteresis

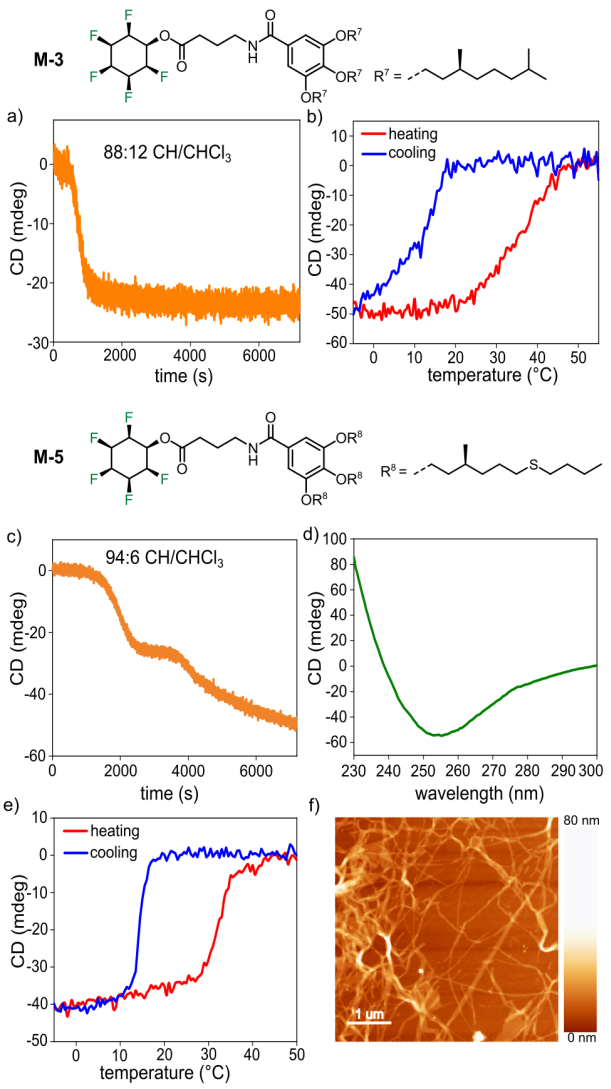

Figure 2 a) CD monitoring (260 nm) of spontaneous polymerization of **M-3** (1.2 mm) in cyclohexane/chloroform (88 : 12 v/v), b) VT-CD (260 nm) experiment of **M-3** (1.2 mm) in cyclohexane/chloroform (88 : 12 v/v) showing hysteresis, c) CD monitoring (260 nm) of spontaneous polymerization of **M-5** (1.2 mm) in cyclohexane/chloroform (94 : 6 v/v), d) full CD spectrum of the spontaneously polymerized **M-5** sample, e) VT-CD (260 nm) experiment of **M-5** (1.2 mm) in cyclohexane/chloroform (94 : 6 v/v) showing hysteresis, f) AFM of the spontaneously polymerized sample of **M-5** (1.2 mm) in cyclohexane/chloroform (94 : 6 v/v); sample deposited by spin-coating on silicon wafer.

for both monomers under these conditions, indicating that polymerization is subject to kinetic control (Figure 2b, e).

During the spontaneous polymerization of both **M-3** and **M-5**, we observed insoluble components in the cuvettes (Figure S1a). However, the CD signal remained unchanged after shaking the cuvette or tilting it upside down. After filtering the sample using a syringe filter of 0.45 µm pore size,

the CD signal vanished completely. In light of a recent review by Meijer and co-workers[19] on reproducibility in supramolecular polymerization, we decided to confirm that monomers **M-3** and **M-5** indeed undergo supramolecular polymerization; we used AFM to study the samples. As shown in Figures 2f and S1b, we observed nanofibers, confirming that the observed CD signal is due to polymerization and the bundling of fibers[20] rather than being an artifact due to linear dichroism (LD) or linear birefringence in the non-homogeneous solution.

Next, we decided to perform controlled polymerization on these monomers. Ultrasound-induced polymerization, seed preparation and seeded polymerization of **M-3** were studied previously, so we focussed on **M-5** in this present study.[15] To our surprise, we were not able to initiate the polymerization of **M-5** reproducibly by applying ultrasound. Instead, precipitate formation was observed during ultrasound irradiation and CD monitoring revealed significant variations between experimental runs under seemingly identical conditions (Figure S2c, d). We believe this finding is noteworthy, because it shows that even a monomer, such as **M-5**, whose polymerization cannot directly be controlled, can still be controlled indirectly by using seeds of a more well-behaved monomer (as we showed in our previous report, in which **M-3** seeds initiated polymerization of **M-5** to give a supramolecular block copolymer[15]).

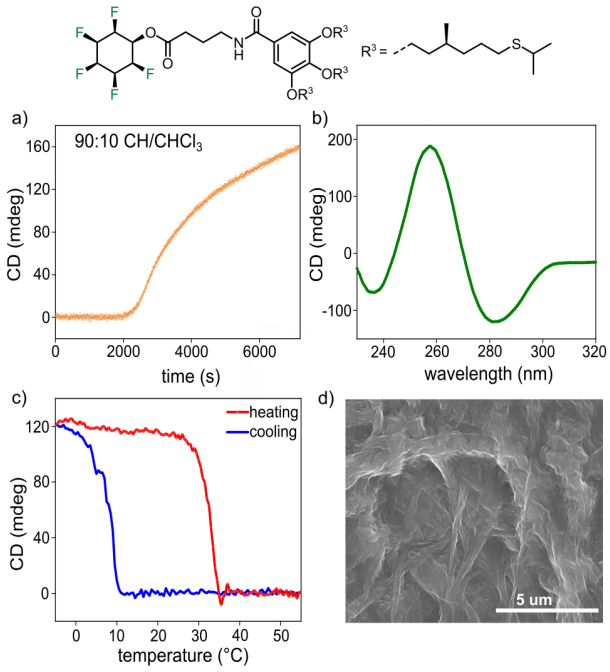

Figure 3 a) CD monitoring (260 nm) of spontaneous polymerization of **M-6** (1.2 mm) in cyclohexane/chloroform (90 : 10 v/v), b) CD spectrum of **M-6** (1.2 mm) in cyclohexane/chloroform (90 : 10 v/v) after spontaneous polymerization, c) VT-CD (260 nm) experiment of **M-6** (1.2 mm) in cyclohexane/chloroform (90 : 10 v/v) showing the hysteresis, d) SEM image of the film formed by spontaneous polymerization; sample was prepared by carefully removing the film from cuvette and depositing on silicon chip.

New Monomers Allowing Spontaneous and Induced Polymerization: M-6 (S^{i}Pr) and M-9 (Urea)

Among the four newly synthesized monomers in this study, two examples (**M-6** and **M-9**) underwent both spontaneous and controlled polymerization and are therefore of special interest in the context of this study and for the wider research field.

Monomer **M-6** with a branched side chain spontaneously polymerized in a solvent composition of 90 : 10 (cyclohexane/chloroform, Figure 3a). A strong positive CD signal was observed at 260 nm (Figure 3b) and a VT-CD experiment showed hysteresis indicating kinetically controlled polymerization (Figure 3c). A two-dimensional insoluble "film" was formed in the cuvette during polymerization. Upon shaking such a cuvette, the CD intensity decreased strongly (Figure S3a). This finding implies that in this case, the observed CD signal contains a dominant contribution from LD/linear birefringence. We repeated this experiment several times, but always observed the same result. To confirm the occurrence of supramolecular polymerization for monomer **M-6**, we investigated the insoluble film using scanning electron microscopy (SEM). SEM images revealed an entangled fibrous morphology (Figure 3d).

In contrast to spontaneous polymerization, formation of an insoluble film was not observed in the ultrasound-induced polymerization in a solvent composition of 86 : 14 (cyclohexane/chloroform). In this solvent system, the molecule is kinetically trapped due to folding for more than 2 hours and therefore showed no sign of polymerization (confirmed by CD spectroscopy, Figure S4a). Sonication for 2 minutes induced the polymerization (Figure S4b). Shaking of the cuvette or filtration using syringe filter (size 0.45 micrometer) did not change the CD signal, implying that the solution is homogeneous and no contribution from LD is present (Figure S4c). The CD signal of the ultrasound-induced sample was different compared to that observed in the spontaneous polymerization. We propose that this difference between CD signals is a result of the formation of different polymorphs.[11] Transmission FT-IR spectra corroborated hydrogen bonding between the amides in both **M-6** materials derived from spontaneous and ultrasound-induced polymerization (Figure S5). AFM of the ultrasound-induced polymers demonstrated formation of nanofibers as a result of polymerization (Figure 4a) and revealed that the diameter of the individual fibres is around 2.4 nm (Figure 4b), which is in accordance with previously observed AFM results on **M-3**.[15]

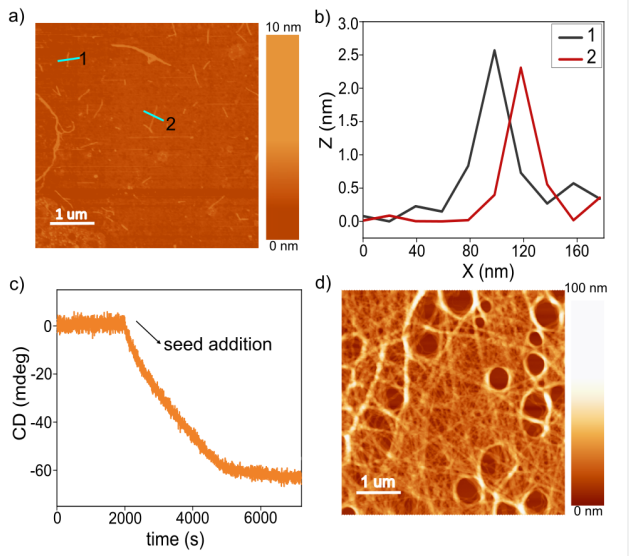

Figure 4 a) AFM image of the sonicated samples after diluting 100 times in cyclohexane; sample deposited by spin-coating on silicon wafer, b) AFM height profiles of the selected fibres, c) CD monitoring of polymerization by addition of seeds to the monomer (50 : 1 monomer to seed ratio, both seed and monomer at 1.2 mm in 84 : 16), d) AFM of the seeded polymer of **M-6** (1.2 mm) in cyclohexane/chloroform (86 : 14 v/v); sample deposited by spin-coating on silicon wafer.

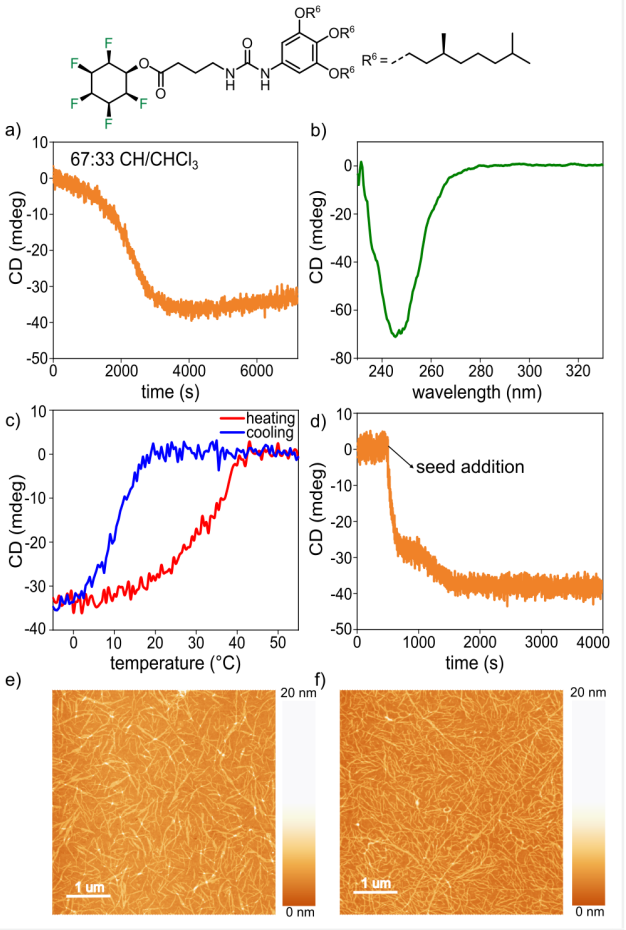

Figure 5 a) CD monitoring (255 nm) of spontaneous polymerization of **M-9** (1.2 mm) in cyclohexane/chloroform (67 : 33 v/v), b) CD spectrum after 5 minutes of sonication of **M-9** (1.2 mm) in cyclohexane/chloroform (63 : 37 v/v), c) VT-CD (255 nm) experiment of **M-9** (1.2 mm) in cyclohexane/chloroform (67 : 33 v/v) showing hysteresis, d) seed-induced polymerization (255 nm) of **M-9** (1.2 mm) in cyclohexane/chloroform (63 : 37 v/v), 50 : 1 monomer to seed ratio, e) AFM image of the seeds prepared by sonication of **M-9** (1.2 mm) in cyclohexane/chloroform (63 : 37 v/v), f) AFM image of the polymer obtained by the addition of seeds to the monomer (50 : 1 monomer to seed ratio, both seed and monomer at 1.2 mm in 63 : 37 cyclohexane/chloroform); samples deposited by spin-coating on silicon wafer.

The sonication-induced polymer was next used as a seed to initiate polymerization. Seeds prepared by short (2-minute) sonication of a 1.2 mm solution of **M-6** in 86 : 14 cyclohexane/chloroform were added to a monomer solution of **M-6** (1.2 mm) in 86 : 14 cyclohexane/chloroform in a monomer to seed ratio of 50 : 1. Polymerization started immediately upon the addition of seeds (Figure 4c, d). This result shows that it is possible to carry out LSP with the new monomer **M-6**.

With monomer **M-6**, we observed changes in the CD signal of spontaneously polymerized material over time. The initially formed film in the cuvette converted (over 1 day at 20 °C) to a more transparent liquid exhibiting a different CD signal (Figure S6a, b). Shaking of the cuvette or filtration of the solution led to disappearance of the CD signal, indicating inhomogeneity of the sample. AFM of the aged sample showed a fibrous morphology (Figure S6c). We propose that these results point toward different pathways in the supramolecular polymerization of **M-6**, where the initially formed kinetically stable species convert to thermodynamically more stable species over time.

M-9 was designed to study the effect of replacing the amide with a urea motif on both polymerization and the kinetically trapped folded state. We found that **M-9** polymerized spontaneously (Figure 5a) in a solvent composition of 67 : 33 (cyclohexane/chloroform). A hysteresis curve was observed by CD spectroscopy during the heating/cooling cycle, indicating kinetically controlled polymerization. When increasing the chloroform fraction in the solvent mixture (63 : 37), we observed no sign of polymerization, as confirmed by CD spectroscopy (Figure S7a). Yet, after sonication for 5 minutes, a pronounced negative CD signal emerged (Figure 5b) as a result of supramolecular polymerization, as confirmed by AFM (Figure 5e). Seeds derived from this sonication-induced polymerization were successfully used to induce the living polymerization of a fresh solution of monomers in a solvent mixture of 63 : 37 (cyclohexane/chlo-

roform; Figure 5d, f). We conclude that monomer **M-9** behaved as an ideal monomer, because both spontaneous and induced polymerization could be carried out and precipitation was absent in either case.

Monomers That Did Not Polymerize: M-7 ($SC_8H_4F_{13}$) and M-8 (SBn)

Two of the new monomers (**M-7** and **M-8**) studied herein did not polymerize into well-defined self-assembled structures. **M-7** was synthesized to study the effect of fluorinated alkyl chains on polymerization and on the morphology of the resulting supramolecular assembly as unusual morphologies were reported by several groups before.[6] Yet, **M-7** was found to precipitate in a solvent composition of 71 : 29 (cyclohexane/chloroform) along with the occurrence of a large negative CD signal after a lag time of 50 minutes (Figure S8a) was observed. Shaking of the cuvette or filtration of the solution led to disappearance of the CD signal and AFM studies did not reveal any fibrous morphology, but images of inconsistent and ill-defined objects (Figure S8b, c).

Similar to **M-7**, monomer **M-8** also did not polymerize in a well-behaved manner in the binary solvent system of cyclohexane and chloroform. Either precipitation (with cyclohexane content exceeding 75%) or no precipitation (with cyclohexane content lower than 75%) was observed and no significant CD signal was observed in both of these scenarios. We attribute these findings to the poor solvation of these molecules due to the presence of fluorinated side chains or aromatic residues that are mismatched with both solvents in the binary mixture of cyclohexane and chloroform. Future work on monomers **M-7** and **M-8** may therefore focus on ternary solvent mixtures or binary solvents including aromatic or fluorous solvents.

Chloride-Induced Depolymerization

Having comprehensively studied the stimuli-induced polymerization of all-*cis*-fluorinated cyclohexanes, we proceeded to study the chemically induced depolymerization of the obtained nanofibers. Because all-*cis* hexafluorocyclohexane was shown to bind anions such as chloride, moderately strong (K_a 400 M^{-1} in acetone),[18] we hypothesized that addition of chloride could depolymerize the nanofibers, essentially by competing with the stacking of fluorinated cyclohexanes (Figure 6a). If successful, such an experiment would further confirm the importance of the all-*cis*-fluorinated cyclohexane motif for the stability of the nanofibers (we had previously shown that a non-fluorinated cyclohexane derivative does not polymerize).[15] To test this hypothesis, we prepared a polymer solution of **M-6** by sonicating a 1.2 mm solution in 86 : 14 cyclohexane/chloroform for 2

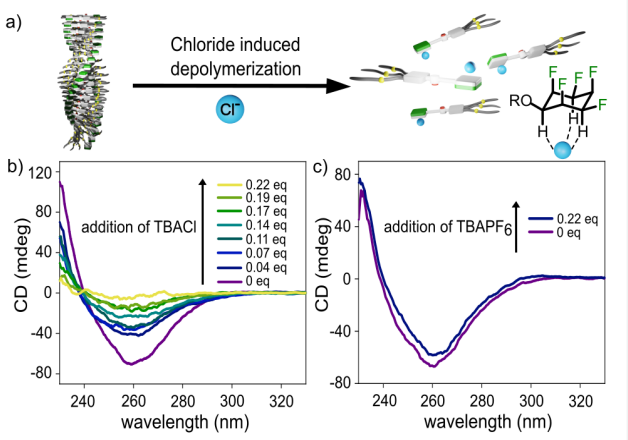

Figure 6 a) Schematic representation of chloride-induced depolymerization of **M-6** polymer, b) sequential addition of 1.2 mm TBACl (86 : 14, cyclohexane, $CHCl_3$) to a 1.2 mm polymer solution of **M-6** (86 : 14, cyclohexane, $CHCl_3$) showing the depolymerization. Upon addition of 0.22 equiv of TBACl, depolymerization completed. c) **M-6** polymer (green) and after adding 0.22 equiv of **$TBAPF_6$** (red), not much change was observed.

minutes. A solution of 1.2 mm TBACl and 1.2 mm **M-6** was prepared in the same solvent as a chloride ion source (the **M-6** was added to TBACl to nullify the dilution effect). As shown in Figure 6b, we found that the polymer solution depolymerized completely upon adding 0.22 equiv of chloride as confirmed by CD spectroscopy. As a control experiment, we added 0.22 equiv of $TBAPF_6$ to the same polymer solution, which led to negligible depolymerization (Figure 6c), in accordance with our previous study.[18] AFM and dynamic light scattering data further corroborate these findings (Figure S9).

Conclusions

We studied the supramolecular polymerization of six monomers (**M-3, M-5–9**) based on the stacking of the all-*cis*-fluorinated cyclohexane moiety. With the exception of **M-7** and **M-8**, all monomers polymerized spontaneously to give relatively well-behaved organic materials and hysteresis curves obtained during heating/cooling cycles clearly show that polymerization is kinetically controlled (Table 1). We propose that **M-7** and **M-8** did not polymerize due to the poor solvation of a peripheral perfluorinated chain or an aromatic ring. Seeded polymerization, which is the most sought-after method, because it allows length control, was achieved for four monomers (**M-3, M-5, M-6, M-9**), yet only three monomers allowed the preparation of seeds by ultrasonication (**M-5** could nevertheless be initiated using seeds of a different monomer). This study shows that the LSP of fluorinated cyclohexanes is not limited to one monomer. Indeed, the new monomer **M-9** whose "folding motif" contains a urea

Table 1 Summary of the polymerization properties of the monomers studied in this work

Molecule studied	Spontaneous polymerization	Induced polymerization			Additional remarks
		Cooling	Ultrasound	Seed	
M-3 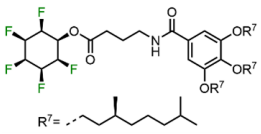	✓[#] CH:$CHCl_3$ 88:12	✓ 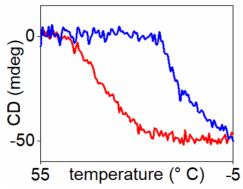	✓	✓	Well-studied monomer in our previous work.[15] Allows doing LSP in a 84:16 CH/$CHCl_3$ solvent system.
M-5 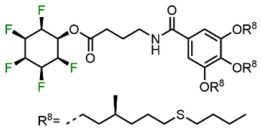	✓[#] CH:$CHCl_3$ 94:6	✓ 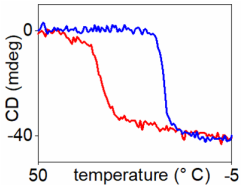	✗	✓	Not possible to prepare seeds of this monomer. It was possible to initiate seeded polymerization by using seeds of **M-3** (leading to block copolymer).
M-6 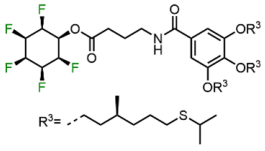	✓[#] CH:$CHCl_3$ 90:10	✓ 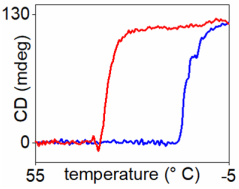	✓	✓	Precipitation due to bundling of fibres during spontaneous polymerization. Allows controlled polymerization and LSP.
M-9 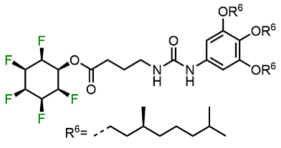	✓ CH:$CHCl_3$ 67:33	✓ 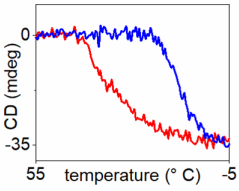	✓	✓	Well-behaved monomer undergoing spontaneous polymerization, controlled polymerization. Also allows doing LSP.
M-7 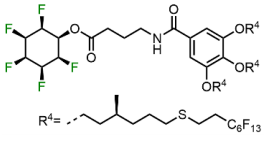	✗	✗	✗	✗	No polymerization due to poor solvation of the monomers by the CH/$CHCl_3$ binary solvent system used in this study.
M-8 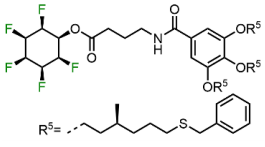	✗	✗	✗	✗	No polymerization due to poor solvation of the monomers by the CH/$CHCl_3$ binary solvent system used in this study.

[#]Precipitate formation due to bundling of fibres during the spontaneous polymerization.

group, instead of an amide, seems to be the most ideal monomer that we identified so far. We also show that the supramolecular polymers of fluorinated cyclohexanes can be depolymerized by the addition of chloride ion. Studies on the use of chloride ion as a sequestrator[21] and dilution-induced supramolecular polymerization[22] are ongoing.

Experimental Section

All commercially available chemicals were purchased from Merck-Sigma Aldrich, TCI Germany, ABCR, Acros Organics, and Alfa Aesar, and were used without further purification. Dry solvents were collected from an MBraun-SPS-800 system. Hydrogenation reactions were carried out in a 50 mL Roth high-pressure autoclave. For detailed experimental procedure and characterization, please refer to the Supporting Information.

Funding Information

This work was supported by the European Union (ERCstg 802 428 "SUPRANET").

Supporting Information

Supporting Information for this article is available online at https://doi.org/10.1055/10.1055/s-0043-1761314.

Conflict of Interest

The authors declare no conflict of interest.

References

(1) Brunsveld, L.; Folmer, B. J. B.; Meijer, E. W.; Sijbesma, R. P. *Chem. Rev.* **2001**, *101*, 4071.
(2) (a) Aida, T.; Meijer, E. W.; Stupp, S. I. *Science* **2012**, *335*, 813. (b) Webber, M. J.; Appel, E. A.; Meijer, E. W.; Langer, R. *Nat. Mater.* **2016**, *15*, 13. (c) Dumele, O.; Chen, J.; Passarelli, J. V.; Stupp, S. I. *Adv. Mater.* **2020**, *32*, 1907247.
(3) (a) Ponnuswamy, N.; Pantoş, G. D.; Smulders, M. M. J.; Sanders, J. K. M. *J. Am. Chem. Soc.* **2012**, *134*, 566. (b) Lynes, A. D.; Hawes, C. S.; Ward, E. N.; Haffner, B.; Möbius, M. E.; Byrne, K.; Schmitt, W.; Pal, R.; Gunnlaugsson, T. *CrstEngComm* **2017**, *19*, 1427. (c) Desmarchelier, A.; Alvarenga, B. G.; Caumes, X.; Dubreucq, L.; Troufflard, C.; Tessier, M.; Vanthuyne, N.; Idé, J.; Maistriaux, T.; Beljonne, D.; Brocorens, P.; Lazzaroni, R.; Raynal, M.; Bouteiller, L. *Soft Matter* **2016**, *12*, 7824.
(4) Cantekin, S.; de Greef, T. F. A.; Palmans, A. R. A. *Chem. Soc. Rev.* **2012**, *41*, 6125.
(5) Besenius, P.; Heynens, J. L.; Straathof, R.; Nieuwenhuizen, M. M.; Bomans, P. H.; Terreno, E.; Aime, S.; Strijkers, G. J.; Nicolay, K.; Meijer, E. W. *Contrast Media Mol. Imaging* **2012**, *7*, 356.
(6) (a) Sasaki N.; Mabesoone, M. F. J.; Kikkawa, J.; Fukui, T.; Shioya, N.; Shimoaka, T.; Hasegawa, T.; Takagi, H.; Haruki, R.; Shimizu, N.; Adachi, S. I.; Meijer, E. W.; Takeuchi, M.; Sugiyasu, K. *Nat. Commun.* **2020**, *11*, 3578. (b) Stals, P. J. M.; Korevaar, P. A.; Gillissen, M. A.; de Greef, T. F.; Fitié, C. F.; Sijbesma, R. P.; Palmans, A. R.; Meijer, E. W. *Angew. Chem. Int. Ed.* **2012**, *51*, 11297. (c) Prasanthkumar, S.; Zhang, W.; Jin, W.; Fukushima, T.; Aida, T. *Angew. Chem. Int. Ed.* **2015**, *54*, 11168.
(7) Wang, X.; Manners, I.; Winnik, M. A. *Science* **2007**, *317*, 644.
(8) (a) Wehner, M.; Würthner, F. *Nat. Rev. Chem.* **2020**, *4*, 38. (b) Mukhopadhyay, R. D.; AJayghosh, A. *Science* **2015**, *349*, 6245. (c) Ghosh, G.; Dey, P.; Ghosh, S. *Chem. Commun.* **2020**, *56*, 6757.
(9) (a) Adelizzi, B.; Aloi, A.; Markvoort, A. J.; Ten Eikelder, H. M. M.; Voets, I. K.; Palmans, A. R. A.; Meijer, E. W. *J. Am. Chem. Soc.* **2018**, *140*, 7168. (b) Jung, S. H.; Bochicchio, D.; Pavan, G. M.; Sugiyasu, K. *J. Am. Chem. Soc.* **2018**, *140*, 10570. (c) Wagner, W.; Wehner, M.; Stepanenko, V.; Würthner, F. *J. Am. Chem. Soc.* **2019**, *141*, 12044.
(10) Ogi, S.; Sugiyasu, K.; Manna, S.; Takeuchi, M. *Nat. Chem.* **2014**, *6*, 188.
(11) (a) Korevaar, P. A.; George, S. J.; Markvoort, A. J.; Smulders, M. M.; Hilbers, P. A.; Schenning, A. P.; De Greef, T. F.; Meijer, E. W. *Nature* **2012**, *481*, 492. (b) Matern, J.; Dorca, Y.; Sánchez, L.; Fernández, G. *Angew. Chem. Int. Ed.* **2019**, *58*, 16730. (c) Langenstroer, A.; Kartha, K. K.; Dorca, Y.; Droste, J.; Stepanenko, V.; Albuquerque, R. Q.; Hansen, M. R.; Sánchez, L.; Fernández, G. *J. Am. Chem. Soc.* **2019**, *141*, 5192. (d) Ogi, S.; Fukui, T.; Jue, M. L.; Takeuchi, M.; Sugiyasu, K. *Angew. Chem. Int. Ed.* **2014**, *53*, 14363. (e) Würthner, F.; Yao, S.; Beginn, U. *Angew. Chem. Int. Ed.* **2003**, *42*, 3247. (f) Yagai, S.; Yamauchi, M.; Kobayashi, A.; Karatsu, T.; Kitamura, A.; Ohba, T.; Kikkawa, Y. *J. Am. Chem. Soc.* **2012**, *134*, 18205. (g) Hifsudheen, M.; Mishra, R. K.; Vedhanarayanan, B.; Praveen, V. K.; Ajayaghosh, A. *Angew. Chem. Int. Ed.* **2017**, *56*, 12634. (h) Wehner, M.; Röhr, M. I. S.; Bühler, M.; Stepanenko, V.; Wagner, W.; Würthner, F. *J. Am. Chem. Soc.* **2019**, *141*, 6092.
(12) (a) Wagner, W.; Wehner, M.; Stepanenko, V.; Ogi, S.; Würthner, F. *Angew. Chem. Int. Ed.* **2017**, *56*, 16008. (b) Fukui, T.; Kawai, S.; Fujinuma, S.; Matsushita, Y.; Yasuda, T.; Sakurai, T.; Seki, S.; Takeuchi, M.; Sugiyasu, K. *Nat. Chem.* **2017**, *9*, 493. (c) Sarkar, A.; Sasmal, R.; Empereur-Mot, C.; Bochicchio, D.; Kompella, S. V. K.; Sharma, K.; Dhiman, S.; Sundaram, B.; Agasti, S. S.; Pavan, G. M.; George, S. J. *J. Am. Chem. Soc.* **2020**, *142*, 7606. (d) Greciano, E. E.; Matarranz, B.; Sánchez, L. *Angew. Chem. Int. Ed.* **2018**, *57*, 4697. (e) Greciano, E. E.; Sánchez. L. *Chem. Eur. J.* **2016**, *22*, 13724. (f) Ma. X.; Zhang, Y.; Zhang, Y.; Liu, Y.; Che, Y.; Zhao, J. *Angew. Chem. Int. Ed.* **2016**, *55*, 9539. (g) Wang, H.; Zhang, Y.; Chen, Y.; Pan, H.; Ren, X.; Chen, Z. *Angew. Chem. Int. Ed.* **2020**, *59*, 5185. (h) Helmers, I.; Ghosh, G.; Albuquerque, R. Q.; Fernández, G. *Angew. Chem. Int. Ed.* **2021**, *60*, 4368. (i) Valera, J. S.; Gómez, R.; Sánchez, L. *Small* **2018**, *14*, 1702437. (j) Aliprandi, A.; Mauro, M.; De Cola, L. *Nat. Chem.* **2016**, *8*, 10. (k) Ogi, S.; Stepanenko, V.; Thein, J.; Würthner, F. *J. Am. Chem. Soc.* **2016**, *138*, 670. (l) Sarkar, S.; Sarkar, A.; George, S. J. *Angew. Chem. Int. Ed.* **2020**, *59*, 19841. (m) Sarkar, S.; Sarkar, A.; Som, A.; Agasti, S. S.; George, S. J. *J. Am. Chem. Soc.* **2021**, *143*, 11777. (n) Sarkar, A.; Sasmal, R.; Das, A.; Agasti, S. S.; George, S. J. *Chem. Commun.* **2021**, *57*, 3937. (o) Sarkar, A.; Sasmal, R.; Das, A.; Venugopal, A.; Agasti, S. S.; George, S. J. *Angew. Chem. Int. Ed.* **2021**, *60*, 18209. (p) Laishram, R.; Sarkar, S.; Seth, I.; Khatun, N.; Aswal, V. K.; Maitra, U.; George,

S. J. *J. Am. Chem. Soc.* **2022**, *144*, 11306. (q) Sasaki, N.; Yuan, J.; Fukui, T.; Takeuchi, M.; Sugiyasu, K. *Chem. Eur. J.* **2020**, *26*, 7840. (r) Singh, A.; Joseph, J. P.; Gupta, D.; Sarkar, I.; Pal, A. *Chem. Commun*. **2018**, *54*, 10730.

(13) (a) Kang, J.; Miyajima, D.; Mori, T.; Inoue, Y.; Itoh, Y.; Aida, T. *Science* **2015**, *347*, 646. (b) Ogi, S.; Stepanenko, V.; Sugiyasu, K.; Takeuchi, M.; Würthner, F. *J. Am. Chem. Soc.* **2015**, *137*, 3300. (c) Ogi, S.; Matsumoto, K.; Yamaguchi, S. *Angew. Chem. Int. Ed*. **2018**, *57*, 2339. (d) Fukaya, N.; Ogi, S.; Kawashiro, M.; Yamaguchi, S. *Chem. Commun*. **2020**, *56*, 12901. (e) Choi, H.; Ogi, S.; Ando, N.; Yamaguchi, S. *J. Am. Chem. Soc*. **2021**, *143*, 2953. (f) Ogi, S.; Fukaya, N.; Arifin; Skjelstad, B. B.; Hijikata, Y.; Yamaguchi, S. *Chem. Eur. J.* **2019**, *25*, 7303. (g) Naranjo, C.; Adalid, S.; Gómez, R.; Sánchez, L.; *Angew. Chem. Int. Ed*. **2023**, *62*, e202218572.

(14) (a) Mishra, A.; Korlepara, D. B.; Kumar, M.; Jain, A.; Jonnalagadda, N.; Bejagam, K. K.; Balasubramanian, S.; George, S. J. *Nat. Commun*. **2018**, *9*, 1295. (b) Jain, A.; Dhiman, S.; Dhayani, A.; Vemula, P. K.; George, S. J. *Nat. Commun*. **2019**, *10*, 450. (c) Endo, M.; Fukui, T.; Jung, S. H.; Yagai, S.; Takeuchi, M.; Sugiyasu, K. *J. Am. Chem. Soc*. **2016**, *138*, 14347. (d) Chakraborty, A.; Ghosh, G.; Pal, D. S.; Varghese, S.; Ghosh, S. *Chem. Sci*. **2019**, *10*, 7345.

(15) Shyshov. O.; Haridas, S. V.; Pesce, L.; Qi, H.; Gardin, A.; Bochicchio, D.; Kaiser, U.; Pavan, G. M.; von Delius, M. *Nat. Commun*. **2021**, *12*, 3134.

(16) (a) Keddie, N. S.; Slawin, A. M. Z.; Lebl, T.; Philp, D.; O'Hagan, D. *Nat. Chem*. **2015**, *7*, 483. (b) Wiesenfeldt, M. P.; Nairoukh, Z.; Li, W.; Glorius, F. *Science* **2017**, *357*, 908.

(17) (a) Pratik, S. M.; Nijamudheen, A.; Datta, A. *ChemPhysChem* **2016**, *17*, 2373. (b) Clark, J. L.; Taylor, A.; Geddis, A.; Neyyappadath, R. M.; Piscelli, B. A.; Yu, C.; Cordes, D. B.; Slawin, A. M. Z.; Cormanich, R. A.; Guldin, S.; O'Hagan, D. *Chem. Sci*. **2021**, *12*, 9712. (c) Poskin, T. J.; Piscelli, B. A.; Yoshida, K.; Cordes, D. B.; Slawin, A. M. Z.; Cormanich R. A.; Yamada, S.; O'Hagan, D. *Chem. Commun*. **2022**, *58*, 7968. (d) Yu, C.; Piscelli, B. A.; Maharik, N. A.; Cordes, D. B; Slawin, A. M. Z.; Cormanich, R. A.; O'Hagan, D. *Chem. Commun*. **2022**, *58*, 12855. (e) Clark, J. L.; Neyyappadadth, R. M.; Yu, C.; Slawin, A. M. Z.; Cordes, D. B.; O'Hagan, D. *Chem. Eur. J.* **2021**, *27*, 16000. (f) Theodoridis, A.; Papamokos, G.; Wiesenfeldt, M. P.; Wollenburg, M.; Müllen, K.; Glorius, F.; Floudas, G. *J. Phys. Chem. B* **2021**, *125*, 3700. (g) Al-Maharik, N.; Kirsch, P.; Slawin, A. M. Z.; Cordes, D. B.; O'Hagan, D. *Org. Biomol. Chem*. **2016**, *14*, 9974. (h) O'Hagan, D. *Chem. Rec.* **2023**, e202300027.

(18) Shyshov, O.; Siewerth, K. A.; von Delius, M. *Chem. Commun*. **2018**, *54*, 4353.

(19) Schnitzer, T.; Preuss, M. D.; van Basten, J.; Schoenmakers, S. M. C.; Spiering, A. J. H.; Vantomme, G.; Meijer, E. W. *Angew. Chem. Int. Ed*. **2022**, *61*, e202206738.

(20) Fukui, T.; Sasaki, N.; Takeuchi, M.; Sugiyasu, K. *Chem. Sci*. **2019**, *10*, 6770.

(21) Vantomme, G.; Ter Huurne, G. M.; Kulkarni, C.; Ten Eikelder, H. M. M.; Markvoort, A. J.; Palmans, A. R. A.; Meijer, E. W. *J. Am. Chem. Soc*. **2019**, *141*, 18278.

(22) (a) Weyandt, E.; Leanza, L.; Capelli, R.; Pavan, G. M.; Vantomme, G.; Meijer, E. W. *Nat. Commun*. **2022**, *13*, 248. (b) Su, L.; Mosquera, J.; Mabesoone, M. F. J.; Schoenmakers, S. M. C.; Muller, C.; Vleugels, M. E. J.; Dhiman, S.; Wijker, S.; Palmans, A. R. A.; Meijer, E. W. *Science* **2022**, *377*, 213. (c) Jansen, S. A. H.; Weyandt, E.; Aoki, T.; Akiyama, T.; Itoh, Y.; Vantomme, G.; Aida, T.; Meijer, E. W. *J. Am. Chem. Soc*. **2023**, *145*, 4231.